CENTER FOR CONNECTED AND AUTOMATED TRANSPORTATION

Final Report #58
September 2023

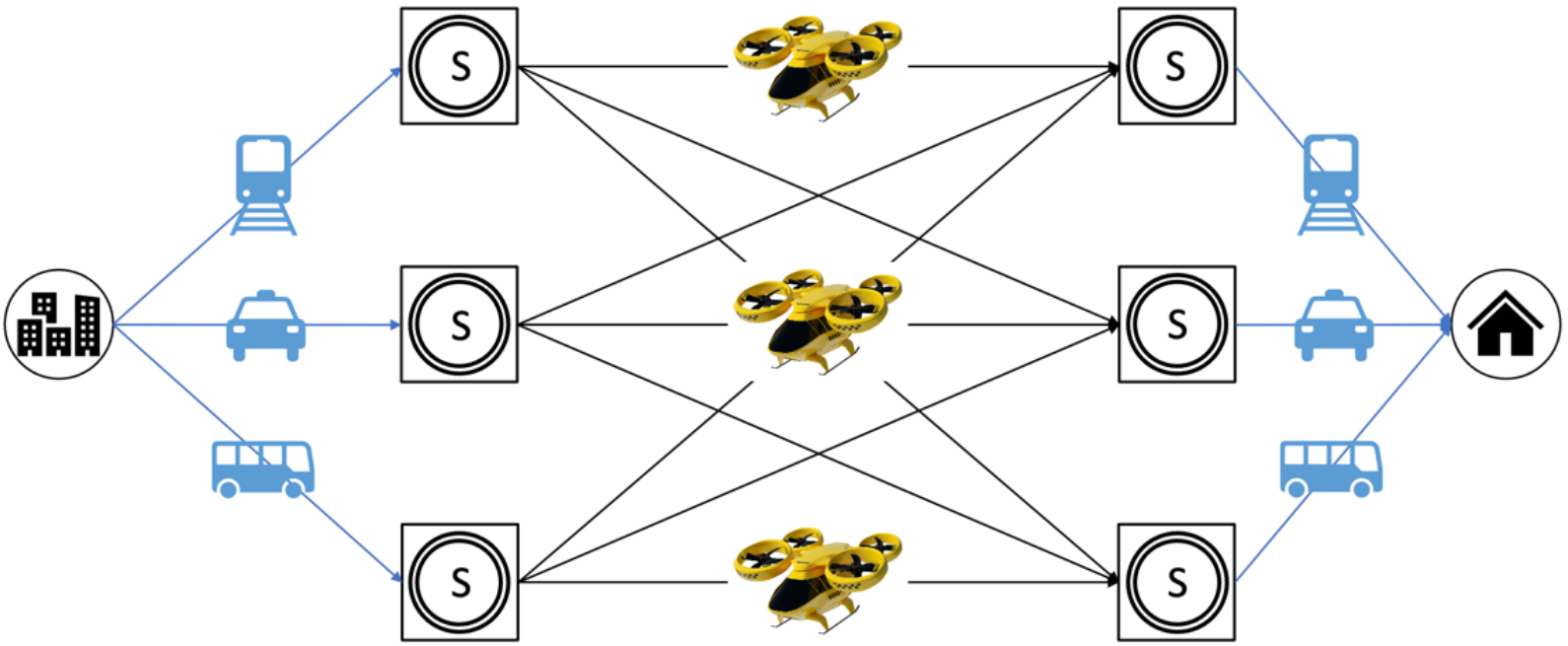

Ride-sharing with Advanced Air Mobility

Shuting Yang
Jiazhen Zhou
Dengfeng Sun
Daniel DeLaurentis

PURDUE UNIVERSITY®

CENTER FOR CONNECTED AND AUTOMATED TRANSPORTATION

Report No. 58 September 2023

Project Start Date: 01/01/2021

Project End Date: 08/31/2023

Ride-sharing with Advanced Air Mobility

By

Shuting Yang
Graduate Researcher

Jiazhen Zhou
Graduate Researcher

Dengfeng Sun
Professor

Daniel DeLaurentis
Professor

Purdue University

ACKNOWLEDGEMENTS AND DISCLAIMER

Funding for this research was provided by the Center for Connected and Automated Transportation under Grant No. 69A3551747105 of the U.S. Department of Transportation, Office of the Assistant Secretary for Research and Technology (OST-R), University Transportation Centers Program. The contents of this report reflect the views of the authors, who are responsible for the facts and the accuracy of the information presented herein. This document is disseminated under the sponsorship of the Department of Transportation, University Transportation Centers Program, in the interest of information exchange. The U.S. Government assumes no liability for the contents or use thereof.

Source of Cover Image: Adapted from Marharyta Marko.

Suggested APA Format Citation:

Yang, S., Zhou, J., Sun, D., and DeLaurentis, D. (2023). Ride-sharing with Advanced Air Mobility, CCAT Report #58, The Center for Connected and Automated Transportation, Purdue University, West Lafayette, IN.

Contacts

For more information:

Samuel Labi, Ph.D.
Purdue University
550 Stadium Mall Drive
HAMP G175B
Phone: (765) 494-5926
Email: labi@purdue.edu

CCAT
University of Michigan
Transportation Research Institute
2901 Baxter Road
Ann Arbor, MI, 48152

uumtri-ccat@umich.edu
(734) 763-2498
www.ccat.umtri.umich.edu

Technical Report Documentation Page

1. Report No. 58	**2. Government Accession No.**	**3. Recipient's Catalog No.**
4. Title and Subtitle Ride-sharing with Advanced Air Mobility		**5. Report Date** September 2023
		6. Performing Organization Code N/A
7. Author(s) Shuting Yang, Jiazhen Zhou, Dengfeng Sun, and Daniel DeLaurentis		**8. Performing Organization Report No.** **N/A**
9. Performing Organization Name and Address Center for Connected and Automated Transportation, Purdue University, 550 Stadium Mall Drive, W. Lafayette, IN 47907; and the University of Michigan Ann Arbor, 2901 Baxter Rd, Ann Arbor, MI 48109		**10. Work Unit No.**
		11. Contract or Grant No. Contract No. 69A3551747105
12. Sponsoring Agency Name and Address U.S. Department of Transportation Office of the Assistant Secretary for Research and Technology 1200 New Jersey Avenue, SE, Washington, DC, 20590		**13. Type of Report and Period Covered** Final report, Jan. 1 2021 –August 31 2023
		14. Sponsoring Agency Code OST-R

15. Supplementary Notes
Conducted under the U.S. DOT Office of the Assistant Secretary for Research and Technology's (OST-R) University Transportation Centers (UTC) program.

16. Abstract
The application of on-demand ridesharing services can improve the efficiency and usage of a metropolitan transportation system. Implementing air taxis service can reduce the number of required aerial vehicles, mitigate air pollution, increase the revenue of the transportation network companies, and boost local economics. In this report, we propose a comprehensive and efficient Mixed Integer Bilinear Programming (MIBLP) model that simultaneously solves two problems: (i) the optimal assignment between the air taxis and the users; and (ii) the optimal path of the air taxis. The study integrates a ground transportation system with air Mobility-on-Demand system using a MIBLP model that aims to minimize the waiting time of the users, operating cost of the air taxis, and the number of unserved ridesharing requests. The study considers dynamic capacities and two statuses (active and idle) of the air taxis, and proposes a batch optimization technique with rolling horizons for large-scale systems. Several scenarios are designed to evaluate the effectiveness and robustness of the proposed model. The results suggest that for a multimodal transportation network with the ridesharing service, optimal assignments between user groups and air taxis, and the optimal path of the air taxis, can be found with within two minutes on average.

17. Key Words Autonomous vehicles, Urban air mobility, Air taxi, Optimization	**18. Distribution Statement** No restrictions.		
19. Security Classif. (of this report) Unclassified	**20. Security Classif. (of this page)** Unclassified	**21. No. of Pages** 38	**22. Price**

TABLE OF CONTENTS

LIST OF FIGURES

LIST OF TABLES

CHAPTER 1 INTRODUCTION

Well-integrated Urban Air Mobility (UAM) has promising advantages in rapid package delivery, fast emergency response, and efficient ridesharing service. UAM envisions a safe and efficient aviation transportation system that will enable automated transportation of passengers and goods within urban and suburban areas [1]. However, a multitude of challenges arise from the implementation of UAM. First, Unmanned Aerial Vehicle (UAV) is out of the scope of the current airspace infrastructure. A new airspace infrastructure is required to be built for this new alternative transportation option. Second, the continued development and incorporation of the Unmanned Aircraft System (UAS) Traffic Management (UTM) into the National Airspace System is required [2]. Third, it is challenging to integrate UAS into the current ground transportation system while ensuring the safety of humans, animals, ground vehicles, and aerial vehicles [3]. Fourth, a real-time risk assessment framework for UAS is required to ensure safety. Fifth, the real-time path planning algorithm for UAV is needed to minimize the operating cost of UAV and avoid accidents, such as the collision between UAVs and the collision between UAVs and obstacles (e.g., birds). Overall, it takes huge efforts to implement UAM.

We aim, in this report, to tackle the third and fifth challenges mentioned above. One of the solutions is to promote the ride-sharing service of the air taxis defined in Table I. The goal of the air taxi service (i.e., the ridesharing service of the air taxis) is to help people move around the city in a quick, safe, sustainable, and cost-effective manner. United Airlines has made one of the most recent air taxi acquisitions; it has already put down a $10 million deposit as part of a $1 billion partnership with Archer Aviation, an air taxi manufacturing company [4]. In 2023, Archer aims to begin mass producing its electric vertical take-off and landing (eVTOL) aircraft which is designed to travel up to 60 miles on a single charge at speeds of up to 150 miles per hour (mph) [5]. In 2024, Archer's goal is to launch the air taxi service to reduce carbon emissions and traffic jams in urban cities such as Los Angeles and Miami [6]. Archer plans to charge $3.00-$4.00 per user per mile. In other words, by taking an air taxi, a user would pay about $50 to travel between Manhattan and JFK International Airport in Queens [6]. Aside from United Airlines, American Airlines and Boeing are also investing heavily in the future of UAM. Wisk was formed in 2019 through a joint venture between Boeing and Kitty Hawk Corp., an eVTOL aircraft manufacturer co-founded by Larry Page (co-founder of Google and Alphabet Inc.). Boeing invested a further $450 million in Wisk, developing pilotless eVTOL aircraft with a capacity of three to four passengers for short-range rides in cities [7]. American Airlines made a $25 million investment in Vertical Aerospace [8]. Vertical Aerospace is another air taxi manufacturing company that is developing VX4, a zero-carbon eVTOL aircraft that can carry four passengers and a pilot and fly at speeds of up to 202 mph over a range of over 100 miles [9]. American Airlines has agreed to pre-order up to 250 aircraft, representing a potential pre-order commitment of $1 billion, and an option to order an additional 100 aircraft [8]. The U.S. Air Force is also involved in the development of the air taxis for military use [7]. Overall, it is promising to launch the air taxi service within the next few years.

The idea of developing the ridesharing service of the air taxis is inspired by the success of the ridesharing service of ground vehicles. Transportation Network Companies (TNCs), such as Uber, Lyft, and Didi, have fundamentally transformed the mobility in many cities by providing on-demand door-to-door transportation through mobile applications [10]. On-demand ridesharing has been known as an effective way to meet dynamic travel needs and reduce air pollution and traffic jams while significantly reducing the number of required vehicles [12], [13]. Agent- based optimization results of New York City Taxi and Limousine Commission (NYC-TLC) database show that the switch from traditional taxis to shared autonomous vehicles does not compromise service quality (in terms of user waiting time) and can reduce the fleet size by 59%. The benefit of ridesharing is significant with increased occupancy rate, decreased total travel distance (up to 55%), and reduced carbon emissions (up to 866 metric tons per day) [13]. Based on the success of the ground Mobility-on-Demand (MoD) systems defined in Table I led by TNCs [14]–[16], it is reasonable to envision the success of the Air Mobility-on-Demand (AMoD) system that incorporates the ridesharing service of the air taxis. The air taxi service extends the application of on-demand door-to-door transportation to on-demand skyport-to-skyport (defined in Table I) transportation. Compared to ground vehicles, air taxis use three-dimensional airspace by adding vertical space to improve the mobility of a transportation system. Additionally, the air taxis are anticipated and designed to be more energy-efficient, safer, and quieter than any modern helicopter [3], [9], [17]. Therefore, the air taxi service will result in positive impacts on the efficiency and usage of the transportation system in urban and suburban areas.

Table 1.1: Common terminologies in air taxi transportation

Term	**Definition**
Mobility-on-Demand (MoD) Systems	MoD systems can provide users with a reliable mode of transportation that is catered to the individual and improves the access of the disable to the mobility, reducing the waiting time and stress associated with travel [11].
eVTOL	Electric vertical takeoff and landing (eVTOL) technology is similar to that of a helicopter, allowing air taxis to lift and land vertically or maneuver at precise vertical angles between the buildings and other obstacles in metropolitan cities [3].
Air Taxis	Small and eVTOL aircraft that are expected to transport on-demand users in metropolitan cities, with an average capacity of four [3].
Vertiport	A large, centralized hub with facilities for customer pick-up or drop-off, charging, maintenance, and several docking stations for air taxis [3].
Vertistop	A site dedicated only for customer pick-up or drop-off, with no support infrastructure, such as charging stations [3].
Skyport	A common term used for referring to both vertiport and vertistop [3].

In this report, the Air Taxi Ridesharing Problem (ATRP) refers to the challenge of efficiently and effectively providing on-demand air taxi service to users. The stakeholders include users, air taxi manufacturing companies (e.g., Volocopter and Joby Aviation), and ridesharing request platform (e.g., Uber Elevate). The goal is to optimize the use of available air taxis and minimize the number of empty seats during flights, while also providing a convenient and affordable mode of transportation for the users. In the ATRP, each user provides an origin-destination pair, and desired departure and arrival time. The users are willing to share flights with others to reduce flight costs but also value convenience and fast travel time. The challenge is to develop algorithms and systems that can assign the users to the air taxis with compatible routes and schedules to minimize the users' travel time and cost. The ATRP involves multiple considerations, such as aircraft scheduling, user matching, route planning, and pricing strategies. It also requires addressing various technical, logistical, regulatory, and economic challenges, such as managing demand variability, ensuring safety and reliability, optimizing operational costs, and complying with regulatory requirements. Overall, solving the ATRP requires a multidisciplinary approach that combines expertise in aviation, transportation, data science, operations research, and economics.

The ATRP is similar to the Dial-a-Ride Problem (DARP) (i.e., an optimization problem that involves designing efficient routes for a fleet of vehicles to serve a set of users with specific pickup and delivery requests [18]). In DARP, each user has a specific pickup location, destination, and time window in which they must be picked up and dropped off. DARP refers to design a set of routes for the ground vehicles to pick up and drop off the users in such a way that the total distance traveled by the ground vehicles is minimized while satisfying the constraints of the problem. The DARP is a computationally complex problem due to its combinatorial nature and the large number of constraints that must be satisfied [18]. The problem becomes even more challenging when additional constraints such as vehicle capacity, time windows, and priority levels are added. The DARP has various practical applications, such as designing transportation services for the elderly or disabled individuals, optimizing school bus routes, or planning parcel delivery routes. Solving the DARP requires sophisticated optimization algorithms and mathematical models that can efficiently generate feasible and optimal solutions, taking into account the various constraints and uncertainties involved.

While both the ATRP and DARP involve optimization and are computationally complex due to the combinatorial nature and large number of constraints, there are several key differences between them.

- Vehicle type: In the ATRP, the vehicles are air taxis, while in the DARP, the vehicles are typically buses, cars, or other modes of ground transportation.

- Mode of transportation: the ATRP involves air transportation, while the DARP typically involves ground transportation.

- Spatial constraints: the ATRP typically has fewer spatial constraints since the UAVs can travel in a straight line between origin and destination points, while the DARP involves

navigating through road networks and dealing with traffic congestion, one-way streets, and other spatial constraints.

- Time windows: In both problems, passengers have specific pickup and delivery time windows. However, in the DARP, the time windows are typically shorter and more restrictive since ground vehicles need to navigate through traffic and may have multiple stops on a single route. In the ATRP, the number of stops of a ridesharing flight is minimized to save the electric energy of the air taxis because the electric energy consumption is much higher during the take-off and landing phase of the air taxis than during the in-flight phase.

- Safety constraints: the ATRP considers safety as an important factor because any collision will result in huge damages to the users, environment, and the air taxi, while the DARP does not emphasize safety because it is easier to recover from ground traffic accidents than aviation accidents and incidents.

Overall, both the ATRP and DARP involve complex transportation optimization challenges, but they differ in terms of the mode of transportation, spatial constraints, time windows, and safety constraints.

The rest of this report is structured as follows. Chapter 2 investigates related research. Chapter 3 defines the multimodal transportation network and formulates the Mixed Integer Bilinear Programming (MIBLP) model. Chapter 4 demonstrates the optimization results and validates the effectiveness and robustness of the proposed MIBLP model. Chapter 5 discusses the study conclusions and future research, and Chapter 6 presents the USDOT performance indicators. The study outcomes and outputs are listed in Chapter 7.

CHAPTER 2 LITERATURE REVIEW

Ground Mobility-on-Demand (GMoD) systems typically provide carsharing, ridesharing, ridesourcing services, and electronic hailing (e-hail) services [19]. Carsharing means that the user can have short-term access to a shared automobile such as Zipcar. Ridesharing, also known as carpooling and vanpooling, involves users that share a vehicle for trips with common origin, common destination, or both, to reduce the number of vehicles on the road. Ridesourcing services provide prearranged and on-demand transportation services. Users relate to drivers of personal vehicles by using smartphone apps, such as Uber. E-hail services allow users to book public transport services through smartphone apps. For example, e-Hail allows a user to use NYC-TLC-licensed apps to hail a yellow taxicab or Street-Hail Livery (green taxi) using metered rates of fare. E-Hail only refers to the yellow and green taxis in New York City. Similar to the ridesourcing services, e-hail apps facilitate electronic payment and real-time matching of users to drivers [19].

In the Air Mobility-on-Demand (AMoD) system, trip origin, destination, and schedule are dictated by the users. The travel time of UAVs is expected to be a fraction of that of cars. We propose a mathematical model for air ridesourcing services that use smartphone apps to connect the users and the unmanned air taxis. The users use smartphone apps to send air taxi requests to the ridesharing request platform which distributes the air taxis to the users and provides the optimal path of the air taxis. Similarly, ground ridesourcing services use smartphone apps to bring passengers in contact with Autonomous Vehicles (AVs) or drivers who typically drive part-time and use their private cars [19]–[21]. Our AMoD system is different from the ground ridesourcing services in the following areas. First, our AMoD system provides real-time matching of the users to the air taxis and does not offer prearranged flights. Second, any ground location can be the origin or destination of the users with the ground ridesourcing services. In our AMoD system, the users can only choose the origin or destination from a fixed set of the locations of available skyports. Third, safety is an important factor in our AMoD because the injuries caused by aviation accidents and incidents are much more severe than those caused by ground traffic accidents.

Published literature on the AMoD system addresses six main problems: (i) air taxi design and configuration [22]–[28]; (ii) demand estimation [29]–[32]; (iii) skyport design and location [33]–[37]; (iv) ride-matching that is the assignment between groups of users and air taxis [38]–[41]; (v) airspace structure and regulations [42]– [48]; and (vi) environmental effects [49]–[51]. In this report, the proposed MIBLP model aims to address the joint problem of Air Taxi Assignment (ATA) and Air Taxi Path Planning (ATPP). We name the joint problem as Air Taxi Assignment and Path Planning (ATAP). The ride-matching or assignment problem has been studied [3]. However, limited published work addresses the path planning problem of the air taxis. With the advancement of the Global Positioning System (GPS) technology and the increasing number of smart devices, several dynamic path planning algorithms that compute multiple possible paths and determine the best path for traffic in a systematic way are proposed in [52]–[64]. The majority of these works present real-time path planning strategies for UAVs without the ridesharing

characteristic (e.g., search-and-rescue UAVs, military UAVs, and parcel delivery UAVs). Future research could focus on adapting these models to develop cost-effective real-time paths according to the number, location, battery level, and maintenance condition of the air taxis, and the information of the users' air taxi requests (e.g., pick-up/drop-off skyport location, pick-up time, and willingness to ridesharing) [3]. After the drop-off of each user (i.e., the completion of each request), dynamic decisions must be made based on the state of the air taxi (e.g., active, idle, under maintenance check, and battery change). The dynamic path planning algorithm of the air taxis is required to ensure the optimality of UAS [3]. In the proposed MIBLP model, two states of the air taxis (i.e., active, and idle) are considered to make dynamic decisions on the assignment and path planning of the air taxis.

The real-time assignment and path planning of ground taxis and ground autonomous taxis have been well studied [65]–[76]. Relatively fewer published articles address real-time assignment and path planning of air taxis. As such, the current study investigated strategies of the GMoD ridesharing problem for references. A majority of the state-of-the-artwork solves (i) the assignment problem between the ground (autonomous) taxis and the users; and (ii) the optimal path problem of the ground (autonomous) taxis separately. Some work only solves the assignment or the optimal path problem. Only the optimal path problem is addressed in [65] by integrating a Mixed Integer Linear Programming (MILP) model to find the optimal paths, a machine-learning model to predict zone-to-zone demand over time, and a Model Predictive Control optimization to relocate idle vehicles. The objective is to serve all requests and minimize the average waiting time, while satisfying the constraints of ride duration and vehicle capacity. The strategy presented in [65] only ensures the optimal paths; the ride-matching results may not be optimal. The assignment problem is solved at first by using one mathematical framework, and then the path planning problem is solved based on the assignment results by using another mathematical framework in [66]. First, potential paths are found based on the origins and destinations of the users and the locations of ground vehicles. Then, the algorithm starts from a greedy assignment and is improved through a constrained integer linear programming model, converging to the optimal assignment over time. Lastly, the optimal paths are determined based on the optimal assignment results [66]. The vehicle assignment and path planning problems are also solved separately in [67].

The path planning problem is solved first by using a Markov decision process considering idle vehicle re-balancing with properly designed states, actions, and rewards [67]. Meanwhile, by sampling the future requests according to the historical probability distribution, the look-ahead decision making is realized via a framework composed of a convolutional Neural Network and a double deep Q-learning module. Lastly, the assignment problem is solved according to the immediate reward and future gains obtained from the vehicle path planning results in [67]. Overall, optimality is not ensured when the assignment problem and the optimal path problem are solved separately because the ride-matching results and the vehicle paths are correlated. When the assignment problem and the path problem are solved separately in [65]–[67], it is uncertain that the combined results of the two separate results (i.e., the optimal assignments and the optimal paths) are the optimal solution of the joint problem.

The assignment and path planning problems of ground (autonomous) taxis are solved in one mathematical model in [73]–[76]. A reservation system for autonomous taxi ridesharing is designed. Autonomous taxi ridesharing schedules and depot locations are optimized in [73]. In the proposed MIBLP model, a reservation system is not considered, and the depot locations of the air taxis are fully determined by the users because of the limited number of available skyports in a metropolitan city. In [75], a Vehicle Shareable Network (VSN) representing the solution space of all possible paths of the autonomous ground taxis is constructed at first. Then, an integer programming model is used to find the optimal assignment and path of the autonomous ground taxis in terms of energy conservation based on the VSN. In particular, the effects of vehicle load (i.e., a ratio of the capacity of a vehicle to the number of passengers) and vehicle type on fuel consumption are considered in the optimization. Note that the ridesharing feature is not considered in [75]. Inspired by [73] and [75], the electric energy consumption of the air taxis during different flight phases is incorporated into the objective function of the proposed MIBLP model.

A ridesharing Integer Linear Programming (ILP) model is designed for a closed community of companies for scheduled commuter and business trips in [74]. It is reasonable to optimize the choice of meeting-points and car parking points because (i) the users can be a rider or a driver; (ii) it is easy to find a parking spot on the ground; and (iii) the users will return to their origins. Comparing the ILP model with our proposed MIBLP model, the MIBLP model does not limit the users to be employees of nearby companies, and no fixed schedules of ridesharing requests are available. Anyone can be the user, so our model is not only designed for commuter and business trips but also for other purposes (e.g., travel). There should be no return restrictions in our model because the users may not return to the take-off skyports. In the ATAP, each user can use different ground transportation modes (e.g., bus, car, and walk) to go to the take-off skyport, and the users may not come back, so there is no need to optimize the car parking point in the MIBLP model. Regarding the meeting-points optimization, the meeting-points in the MIBLP model are the locations of skyports. The location of a skyport is dependent on the noise level of the air taxis, the available area of skyport construction, the distance between the skyport and busy areas in a city, and government regulations [33]–[37]. Therefore, the meeting-points cannot be any locations and so cannot be optimized based on the air taxi requests in the MIBLP model. The skyport design and location is another research focus of the AMoD system. In this report, we only focus on the air taxi assignment and path planning problems and assume that the locations of skyports are known and fixed.

There are several challenges to formulate the mathematical model of the air taxi service. First, by integrating aerial and ground transportation systems, the computational complexity will increase accordingly. The model needs to include different sets of variables to differentiate between the ground transportation problem and the air transportation problem. The ground ridesharing service uses any location as an origin or destination, whereas the air taxi service will use existing infrastructure, such as airports and helipads, or newly constructed skyports. The locations of the skyports require the users to use ground transportation tools first to reach the take-off skyports of the air taxis, then take the air taxis to the users' requested landing skyports, and

finally use ground transportation tools again to reach the users' final destinations on the ground. Note that a detailed explanation of the multimodal transportation network is presented in Section III-A. The multimodal transportation network implies that different sets of variables need to be considered in the mathematical model. Second, it is challenging to solve the real-time assignment problem of the air taxis by using a mathematical model. The assignment results affect the air taxis' operating cost and the users' travel cost including ground transportation fare, flight fare, and time cost. Thus, the underlying combinatorial nature of the assignment problem between the air taxis and the users is challenging to be accounted into the mathematical model when the problem size is huge. Third, the other challenge is to find the optimal and collision-free paths of the air taxis. The objective is to minimize the operating cost of the air taxis, to guarantee the service quality, the aerial transportation efficiency, and the safety of the air taxis and the users. Thus, it is important to account for not only the optimal paths but also the collision-free paths of the air taxis in the mathematical model. In sum, the underlying computation framework of the air taxi service is crucial and complicated. We aim to propose a mathematical model that can not only efficiently assign the air taxis to the users but also efficiently find the optimal paths of the air taxis.

The study combines ATA and ATPP problems for two reasons. First, the stakeholders of ATA and ATPP problems are users, air taxi manufacturing companies and ridesharing request platform. ATA and ATPP problems are both related to revenue. Non-optimal assignment and paths of the air taxis will lead to longer flight time which increases the operating cost of air taxis and decreases the service quality of TNCs. Second, from the analytical perspective, the optimality of distributing and using air taxis is ensured by solving the joint problem (ATAP). When ATPP problem is solved before ATA problem, if there are many new air taxi requests from skyport A to skyport B at time *t*, the pre-solved paths will not work in this case due to the capacity limit of each route and the availability of air taxis at skyport A at time *t*. If not, many air taxis are not available at skyport A, the waiting time of the users will increase, leading to low service quality. Another case is that when ATA problem is solved before ATPP problem, if the pre-solved assignment is that at time *t*, air taxi 1 is assigned to user 1 (from skyport A to B), and air taxi 2 is assigned to user 2 (from skyport A to B), the current location of air taxi 1 and 2 is skyport A and C respectively. Assume that the available capacity of air taxi 1 is two at time t, the optimal assignment should be air taxi 1 is assigned to both user 1 and 2 so that air taxi 2 does not need to fly from skyport C to skyport A first to pick up user 2 and then fly to skyport B. In this case, the optimal paths based on the non-optimal air taxi assignments become non-optimal. In sum, it is beneficial to solve the joint problem, ATAP, to ensure optimality.

Overall, compared to other works, there are three important and distinct features of our MIBLP model: (i) the integration between the ground transportation system and the AMoD system; (ii) the combination of air taxi assignment and path planning problems; and (iii) the electric energy consumption of air taxis during different flight phases. The main contributions of this report are: (i) to the best of our knowledge, this is one of the first works that focuses on the joint problem, ATAP, and integrates the ground transportation system with the AMoD system; (ii) a clear definition of the multimodal transportation network is demonstrated; (iii) a novel MIBLP model

is proposed to efficiently solve ATAP considering the electric energy consumption of the air taxi during different flight phases (take-off, in-flight, and landing); and (iv) the active and idle statuses of the air taxis are considered in the MIBLP model.

CHAPTER 3 METHODOLOGY

3.1. Multimodal Transportation Network

The formulation of the multimodal transportation network with the ridesharing service (shown in Figure 1) is composed of the following six steps:

- Step 1: Each user starts at any ground location and chooses one out of the six ground transportation methods: (i) G_{m_1} = walk; (ii) G_{m_2} = bicycle; (iii) G_{m_3} = motorcycle; (iv) G_{m_4} = subway; (v) G_{m_5} = bus; (vi) G_{m_6} = car
- Step 2: Each user arrives at the desired take-off skyport by using the ground transportation method chosen in step 1. The user submits an air taxi ridesharing request that includes (i) the take-off skyport; (ii) request submit time; (iii) the landing skyport; (iv) maximum waiting time for pick-up (latest pick-up time); and (v) maximum trip time for drop-off (latest drop-off time).
- Step 3: The ridesharing service platform/provider receives the submitted requests and then uses the proposed MIBLP model to assign idle air taxis to desired users and generate optimal paths for the assigned air taxis, namely active air taxis.
- Step 4: Each active air taxi will take off after the last assigned user arrives at the take-off skyport.
- Step 5: Each active air taxi follows its optimal flight path and drops off onboard users (passengers). After all passengers are dropped off, its status becomes idle.
- Step 6: Each dropped-off user chooses one out of the six ground transportation methods again to go to the user's ground destination.

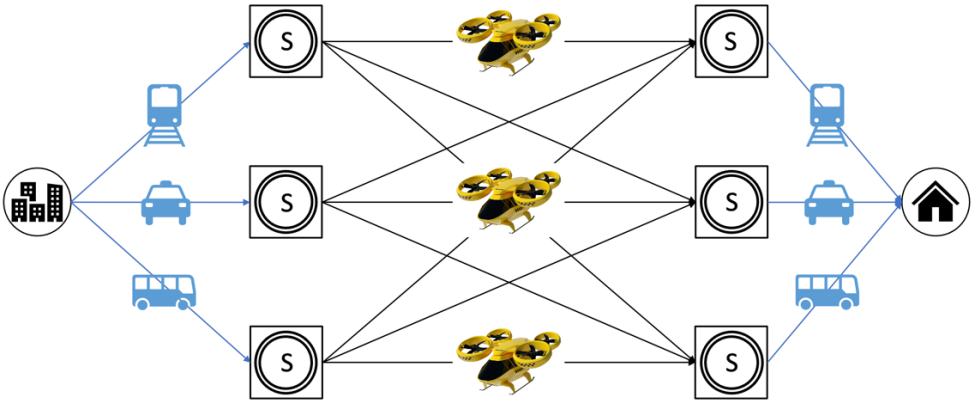

Figure 1: Illustration of the multimodal transportation network; the 3D illustration of the yellow air taxi is credited to Marharyta Marko [77]

3.2. Model Formulation

Since the AMoD system is still in the development phase, there are lots of uncertainties and no unified regulations. We are in the exploration process too. To the best of our knowledge, no work has been proposed to address the ATAP by using one mathematical model. Considering the joint problem ensures the optimality of the optimization results in a systematic way. In this report, we propose a MIBLP model that solves the ATAP while minimizing the waiting time of the users, the operating cost of the air taxis, and the number of unserved ridesharing requests. In the MIBLP model, the location of skyports is fixed and predetermined due to the limited space and regulations of building skyports. The set of available routes is the airspace above the city. We need to deliver users within their maximum waiting time and arrival time. We do not allow passengers to change air taxis during a trip because the take-off and landing of the air taxi require lots of electric energy compared to the in-flight electric energy consumption. We aim to minimize the times of the air taxi take-off and landing.

In this report, we integrate the ground transportation system with the AMoD system. We assume that the speed of ground vehicles is constant. The users can choose any ground transportation methods to travel from ground origins to take-off skyports and from landing skyports to ground destinations. Note that the air taxi request time of each user (i.e., t_{r_p}) is the time that the user arrives at the user's take-off skyport. In the proposed MIBLP model, the starting time of each request is the time when each user arrives at the take-off skyport. The travel time of each trip for each user is from the arrival time of each user's take-off skyport to the arrival time of each user's landing skyport. We assume that (i) the planning horizon is long enough for the problem to be feasible; (ii) each air taxi always has full battery and remains in a good condition so it can take off at any time; (iii) the electric energy consumption of the air taxi take-off and landing are approximately the same. Note that the configuration, infrastructure, and airspace regulations of the air taxis have not been unified or fully developed [3]. Thus, our model does not consider the flight dynamics of the air taxi and so does not account for the exact vertical take-off and landing time of the air taxi.

1) *Notations and Parameters Definitions*: We first define the notation and parameters required to describe the MIBLP model.

- **V** = {1,..., v}: set of air taxis;
- **P** = {1,..., p}: set of users;
- **T** = {0,..., t ,..., $Tmax$ }: set of time steps;
- **R** = {1,..., r}: set of ridesharing requests;
- **G** = {1,..., g}: set of ground locations;
- G_M = {G_{m1},..., G_{m2}}: set of ground transportation methods;
- **S** = {1,..., i}: set of skyport;

- $\mathbf{A} = \{i \rightarrow j\}$: set of arcs between skyport $i \in \mathbf{S}$ and skyport $j \in \mathbf{S}$;
- r_p: the request $r \in \mathbf{R}$ sent by the user $p \in \mathbf{P}$;
- $t_{r_p} \in \mathbf{T}$: the starting time of request $r \in \mathbf{R}$ sent by the user $p \in \mathbf{P}$;
- $t_{w_p} \in \mathbf{T}$: the maximum waiting time (i.e. the latest pick-up time) of the user $p \in \mathbf{P}$;
- $t_{m_p} \in \mathbf{T}$: the maximum onboard time (i.e. the latest drop-off time) of the user $p \in \mathbf{P}$;
- $t_0 \in \mathrm{N}$: the initial time step of an optimization;
- $\mathrm{T_{max}} \in \mathrm{N}^+$: the maximum time step of $t \in \mathbf{T}$;
- $\mathrm{C_v} \in \mathrm{N}^+$: the vehicle capacity of an air taxi $v \in \mathbf{V}$;
- $\mathrm{C_{ij}} \in \mathrm{N}^+$: the path capacity between skyport $i \in \mathbf{S}$ and skyport $j \in \mathbf{S}$;
- $\mathrm{t_{ij}} \in \mathrm{N}^+$: the travel time between skyport $i \in \mathbf{S}$ and skyport $j \in \mathbf{S}$;
- $M \in \mathrm{N}^+$: a very large positive integer;
- $\alpha_{ij} \in \mathrm{N}^+$: the operating cost of travelling between skyport $i \in \mathbf{S}$ to skyport $j \in \mathbf{S}$;
- $\beta \in \mathrm{N}^+$: the penalty of an unserved request;
- $\mathrm{O_v} \in \mathbf{S}$: set of the initial location of each air taxi $v \in \mathbf{V}$;
- $O_{g_p} \in \mathrm{S}$: set of the ground origin of the user $p \in \mathbf{P}$;
- $D_{g_p} \in \mathbf{S}$: set of the ground destination of the user $p \in \mathbf{P}$;
- $O_{r_p} \in \mathbf{S}$: set of the take-off skyport of each request $r \in \mathbf{R}$ sent by the user $p \in \mathbf{P}$;
- $D_{r_p} \in \mathbf{S}$: set of the landing skyport of each request $r \in \mathbf{R}$ sent by the user $p \in \mathbf{P}$.

Note that each request $r \in \boldsymbol{R}$ includes the following information: $\mathrm{r_p}$, t_{r_p}, t_{w_p}, t_{m_p}, $o_{r_p} \in O_{r_p}$, and $d_{r_p} \in D_{r_p}$.

2) *Decision Variables*: The values of the following decision variables are optimized.

$$x_{v_i t} = \begin{cases} 1, & \textit{if vehicle } v \textit{ appears on skyport } i \textit{ at time } t \\ 0, & \textit{otherwise} \end{cases}$$

$$x_{v_{ij} t} = \begin{cases} 1, & \textit{if vehicle } v \textit{ travels from skyport } i \textit{ at skyport } j \textit{ starting at time } t \\ 0, & \textit{otherwise} \end{cases}$$

$$a_{vp} = \begin{cases} 1, & \textit{if vehicle } v \textit{ is assigned to user } p \textit{ and picked up at } p\textit{'s requested take-off skyport} \\ 0, & \textit{otherwise} \end{cases}$$

3.3. Air Taxi Mixed Integer Bilinear Programming (MIBLP) Model

1) *Objective Function*: In this report, the objective function is composed of three components.

$$Min: J = w_1 J_1 + w_2 J_2 + w_3 J_3 \quad (1)$$

where J_1, J_2, and J_3 represent the waiting time of the users, the operating cost of the air taxis, and the penalty of the unserved requests, respectively; w_1, w_2, and w_3 are the weights of the three cost functions that are used to make w_1J_1, w_2J_2, and w_3J_3 have the same unit, \$. The mathematical expressions of J_1, J_2, and J_3 are shown below.

$$J_1 = \sum_{v\in V,\, p\in P,\, r\in R,\, i\in O_r} \sum_{t=t_{r_p}}^{T_{\max}} (t - t_{r_p}).a_{vp}.x_{v_i t} \quad (2)$$

$$J_2 = \sum_{v\in V,\, i,\, j\in S,\, t\in T} x_{v_{ij} t}.(2\alpha_{ii} + \alpha_{ij}) \quad (3)$$

$$J_3 = \sum_{p\in P}[(1 - \sum_{v\in V} a_{vp}).\beta] \quad (4)$$

The stakeholders of ATAP are users, air taxi manufacturing companies, and ridesharing request platform. The overall goal is to maximize the profits of the stakeholders. We aim to minimize the waiting time of the users (J_1) and the penalty of the unserved requests (J_3) to maintain high service quality so that the users are highly satisfied, and so they will bring more users to the ridesharing request platform in the future. In the long run, both the air taxi manufacturing companies and the ridesharing request platform vendor will make more profits from higher service quality and demand. By minimizing the operating cost of the air taxis (J_2), the number of the air taxi take-off and landing times and the duration of the air taxi flight time are minimized so that the stakeholders can make more profit by minimizing the operating cost of the air taxis.

2) *Constraints*: *We require the following set of constraints to be satisfied:*

$$x_{v_i t} \in \{0,1\} \qquad \forall v \in V, i \in S, t \in T \quad (5)$$

$$x_{v_{ij} t} \in [0,1] \qquad \forall v \in V, i, j \in S, t \in T \quad (6)$$

$$a_{vp} \in \{0,1\} \qquad \forall v \in V, p \in P \quad (7)$$

$$x_{v_i t_0} = 1 \qquad \forall v \in V, i \in O_v \quad (8)$$

$$\sum_{i\in S} x_{v_i t} \le 1 \qquad \forall v \in V, t \in T \quad (9)$$

$$\sum_{v \in V} a_{vp} \leq 1 \qquad \forall p \in P \qquad (10)$$

$$\sum_{p \in P} a_{vp} \leq C_v \qquad \forall v \in V \qquad (11)$$

$$\sum_{t=t_{r_p}}^{\min(t_{r_p}+t_{w_p},T_{\max})} x_{v_i t} \geq a_{vp} \qquad \forall v \in V, p \in P, i \in O_r \qquad (12)$$

Equations (5) and (7) ensure the decision variables, x_{vit} and a_{vp} are binary variables. Equation (6) ensures that $x_{v_{ij}t}$ is a continuous variable between 0 and 1 to account for rounding errors and reduce optimization time. Equation (8) specifies the initial location of the air taxis. Equation (9) ensures that at time step *t*, each air taxi appears on at most one skyport. An air taxi cannot appear on more than one skyport simultaneously. Equation (10) ensures that each user can only be paired with at most one air taxi. Equation (11) ensures that each air taxi will not be overloaded. Equation (12) ensures that each air taxi can pick up its assigned user(s) after the air taxi ridesharing request time of its assigned user(s) and before the latest pick-up time of its assigned user(s).

$$\sum_{\tau=t+1}^{\min(t_{r_p}+t_{m_p},T_{\max})} x_{v_j \tau} - \left[x_{v_i t} + a_{vp} \right] \geq -1 \qquad \forall i \in O_r, j \in D_r, v \in V, p \in P, t \in T \qquad (13)$$

$$\sum_{v \in V} x_{v_{ij} t} \leq C_{ij} \qquad \forall i, j \in S, t \in T \qquad (14)$$

$$x_{v_i t} + x_{v_i t} \left[\sum_{\tau=t+1}^{\min(t+1+t_{ij},T_{\max})} x_{v_j \tau} \right] \leq 1 \qquad \forall v \in V, p \in P, t \in T, i, j \in S, i \neq j \qquad (15)$$

$$x_{v_i t} \left[\sum_{\tau=t+1}^{T_{\max}} \max(0, x_{v_j \tau} - \sum_{k \in S} \sum_{\tau'=t+1}^{\tau} x_{v_k \tau'}) \right] \leq x_{v_{ij} t} \qquad \forall v \in V, p \in P, t \in T, i, j, k \in S, i \neq j \qquad (16)$$

Equation (13) ensures that an in-service air taxi must drop off every onboard user within every onboard user's maximum trip time to be considered as a successful completion of its assigned ridesharing request(s). Equation (14) ensures that the number of air taxis flying between two different skyports will not exceed the predetermined path capacity between these two skyports. Equation (15) ensures that the travel time between one skyport and another is considered for the air taxis. Equation (16) ensures that x_{vijt} is a binary variable.

Bilinear inequality is NP-hard and hence it cannot be solved by polynomial time algorithms [78], [79]. Although Gurobi supports constraints containing bilinear terms [80], the computation time is still too long. To increase the computation efficiency of the proposed MIBLP model, bilinear constraints (i.e., Equations (15) and (16)) are transformed into linear constraints by using

the big M method [81]–[83]. Equation (15) is transformed into the form shown in Equation (17). Equation (16) is transformed into the form shown in Equation (18).

$$0 \le \left[\sum_{\tau=t+1}^{\min(t+1+t_{ij},T_{\max})} x_{v_j\tau} \le M(1-x_{v_it}) \right] \qquad \forall v \in V, p \in P, t \in T, i, j \in S, i \ne j \qquad (17)$$

$$x_{v_{ij}t} \le \left[\sum_{\tau=t+1}^{T_{\max})} \max(0, x_{v_j\tau} - \sum_{k \in S} \sum_{\tau'=t+1}^{\tau} x_{v_k\tau'} \right] \le M(1-x_{v_it}) + x_{v_{ij}t} \qquad \forall v \in V, p \in P, t \in T, i, j, k \in S, i \ne j \qquad (18)$$

3) Batch Optimization:

As we mentioned in Section III-A, the air taxi request time is dependent on the ground transportation time. The MIBLP model collects air taxi requests every ΔT, so the requests are split into batches based on ΔT. A guideline to choose the value of ΔT is that the computation time (CPU time) of each batch is much less than ΔT so that the users can receive air taxi assignment information within a short time and be picked up by their corresponding air taxis within their maximum waiting time. By setting relatively small ΔT (i.e., $\Delta T \le 5$ minutes), the CPU time of each batch is less than around 1 minute. Now, we have achieved the real-time air taxi assignment task with the application of batch optimization and rolling horizons.

CHAPTER 4 RESULTS

In this section, we present and discuss the optimization results of the MIBLP model formulated in Section III-B. To assess the performance of the proposed approach, we compare the results of solving the MIBLP problem without (w/o) and with (w/) batch optimization in Gurobi Optimizer with an academic license [80]. To evaluate the computation performance, we present the optimized results on random instances. All optimizations are run on a computer with an Apple M1 Pro Chip with 10-core CPU, 16-core GPU, 16-core Neural Engine, and 16 GB of RAM.

4.1. Example Scenario w/o Batch Optimization

Take a small-scale scenario as an example. There are 3 air taxis (V1, V2, and V3), 4 users (P1,..., P4), 4 ridesharing requests (R1,..., R4), and 6 skyports (S1,..., S6). The air taxi passenger capacity (i.e., C_v) is two for all air taxis. The values of the parameters are: $w_1 = 2$, $w_2 = 1$, $w_3 = 1$, $t_0 = 0$, $Tmax = 15$, $M = 5e9$, and $\beta = 2e5$. The received requests are shown in Table II. The operating cost and travel time between every two skyports are preassigned. The MIBLP model is optimized for 16 time steps, T = {0,1,2..., *t*,..., 15}. Each time step *t* in the optimization is equal to 1 minute in the real world. The computation (CPU) time of this scenario is around 1.54 seconds. The objective value of *J* in Equation (1) is 65. All users are picked up and dropped off as requested in a timely manner. According to Table IV, all users are picked up before the latest pick-up time (i.e., $tr_p + tw_p$) and dropped off before the latest drop-off time (i.e., $tr_p + tm_p$). The assignment results, optimal paths, and timeline of the air taxis are demonstrated in Tables III and IV and Figure 2.

Table 4.1: Air taxi ridesharing requests received

User	Take-off Skyport	Landing Skyport	t_{r_p}	t_{w_p}	t_{m_p}
P1	S1	S2	1	6	11
P2	S3	S5	3	8	12
P3	S4	S3	2	4	8
P4	S5	S2	1	3	5

Table 4.2: Optimal assignments of the air taxis

Air Taxi	Users
V1	P4
V2	P1
V3	P2, P3

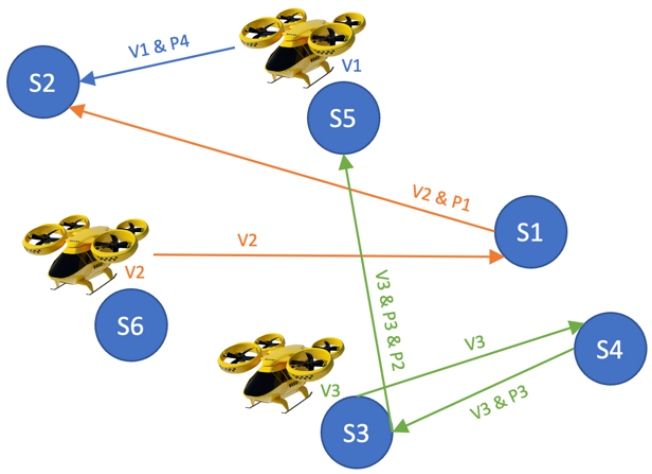

Figure 2: Optimal paths of three air taxis are illustrated visually. The initial locations of V1, V2, and V3 are S5, S6, and S3, respectively. The optimal paths of V1, V2, and V3 are shown in blue, orange, and green, respectively.

Table 4.3: Timeline of the air taxis

Time Step	Air Taxis
0	V1 is at S5; V2 is at S6; V3 is at S3.
1	V1 picks up P4 at S5. V2 is flying from S6 to S1. V3 is flying from S3 to S4.
2	V1 is flying from S5 to S2. V2 is flying to S1 | V3 is flying to S4.
3	V1 lands and drops off P4 at S2; R4 is complete. V2 is flying to S1 | V3 picks up P3 at S4.
4	V2 picks up P1. V3 is flying from S4 to S3.
5	V2 is flying from S1 to S2. V3 is flying to S3.
6	V2 is flying to S2. V3 lands and drops off P3 at S3; R3 is complete. V3 picks up P2 at S3.
7	V2 is flying to S2. V3 is flying from S3 to S5.
8	V2 is flying to S2. V3 is flying to S5.
9	V2 lands and drops off P1 at S2; R1 is complete. V3 is flying to S5.
10	V3 lands and drops off P2 at S5; R2 is complete.
11~15	V1 and V2 stays at S2. V3 stays at S5.

4.2. Computation Efficiency

In order to evaluate the computation efficiency of our model, the numbers of the air taxis and the users are varied; the number and the location of the skyports remain the same so that the air taxis are operated in the same traffic region. Based on Table V, as the system dimension (i.e., the number of variables) increases, the computation (CPU) time increases. It takes about 29 minutes to solve the scenario including 15 air taxis and 30 users without the use of the batch optimization according to Table V. Due to the long CPU time, we propose the rolling-horizon batch optimization technique explained in Section III-C3 to solve large-scale problems.

With the rolling-horizon batch optimization technique, the average CPU time of the scenario including 15 air taxis and 30 users is about 2 minutes. The average CPU time of this scenario is decreased by 92.8 % according to Tables VI to IX. Random instances with different numbers of air taxis and users are optimized to evaluate the computation efficiency of the MIBLP model without and with batch optimization. The locations and number of skyports are fixed. The detailed optimization results without batch optimization are shown in Tables VI and VII.

The detailed optimization results with batch optimization are shown in Tables VIII and IX. For each instance name, (i) the number in front of "AT" refers to the number of air taxis; (ii) the number in front of "P" refers to the number of users; (iii) "R1" refers to a relaxed time window (i.e., large values of tw_p and tm_p); (iv) "R2" refers to a tight time window (i.e., small values of tw_p and tm_p); and (v) the number after "R1" or "R2" is used to distinguish the random instances with the same numbers of air taxis and users but with different initial locations and passenger capacities of the air taxis, and different air taxi requests of the users (e.g., take-off and landing skyport, tw_p , and tr_p).

"Service Rate" refers to the percent of served users with respect to the total number of users in each instance. "Cost" is equal to J, the objective function value shown in Equation (1) when the service rate is 100%. When the service rate is less than 100%, J_3 is equal to a huge number. To understand the other two objectives, "Cost" is equal to the sum of J_1 and J_2 in Tables VI to IX when not all air taxi requests are served. "Gap" refers to the optimality gap in Gurobi. The closer the gap is to zero, the better the solution is. "Optimization Horizon" refers to the optimization time in Gurobi. "CPU Time" refers to the computation time of each instance in Gurobi. The computation time limit is set to 2 hours (7200 seconds) in Gurobi.

Table 4.4: Optimization results of scenarios with different problem scales w/o batch optimization

Number of Air Taxis	Number of Users	Number of Skyports	CPU Time [s]
1	2	6	12.11
2	4	6	108.52
4	6	6	77.23
8	15	6	306.22
15	30	6	1765.94
50	100	6	>7200
200	500	6	>7200

Table 4.5: Optimization results of MIBLP w/o batch optimization w/ relaxed time windows

	MIBLP w/o BO						
Name	β	M	Cost ($)	Service Rate (%)	Gap (%)	Optimization Horizon (min)	CPU Time (s)
1AT2P_R1_1	2E+05	2E+03	325	100	0	31	6.46
1AT2P_R1_2	2E+05	2E+03	226	100	0	16	1.08
1AT2P_R1_3	2E+05	2E+03	228	100	0	17	1.34
2AT4P_R1_1	2E+07	2E+05	543	100	0	28	51.00
2AT4P_R1_2	2E+05	2E+10	741	100	0	32	20.27
2AT4P_R1_3	2E+05	2E+10	763	100	0	38	40.51
4AT6P_R1_1	2E+05	2E+10	857	100	0	38	273.78
4AT6P_R1_2	2E+05	2E+10	745	100	0	21	53.50
4AT6P_R1_3	2E+05	2E+10	747	100	0	18	54.17
8AT15P_R1_1	2E+15	2E+10	6132	100	0	53	551.28
8AT15P_R1_2	2E+15	2E+10	7840	100	0	65	726.70
8AT15P_R1_3	2E+15	2E+10	4232	100	0	58	366.15
15AT30P_R1_1	2E+15	2E+10	8570	100	0	49	204.05
15AT30P_R1_2	2E+20	2E+10	10009	100	0	61	513.16
15AT30P_R1_3	2E+20	2E+10	8153	100	0	54	277.76
50AT100P_R1_1	2E+30	2E+10	inf	0	x	64	>7200
50AT100P_R1_2	2E+30	2E+10	inf	0	x	63	>7200
50AT100P_R1_3	2E+30	2E+10	inf	0	x	62	>7200
100AT500P_R1_1	2E+30	2E+10	inf	0	x	64	>7200
100AT500P_R1_2	2E+30	2E+10	inf	0	x	63	>7200
100AT500P_R1_3	2E+30	2E+10	inf	0	x	62	>7200
Average			**3341**	**71**	**0**	**46**	**>7200**

Table 4.6: Optimization results of MIBLP w/o batch optimization w/ tight time windows

	MIBLP w/o BO						
Name	β	M	Cost ($)	Service Rate (%)	Gap (%)	Optimization Horizon (min)	CPU Time (s)
1AT2P_R2_1	2E+05	2E+03	315	100	0	46	59.44
1AT2P_R2_2	2E+05	2E+03	329	100	0	15	0.44
1AT2P_R2_3	2E+05	2E+03	315	100	0	20	3.90
2AT4P_R2_1	2E+05	2E+10	847	100	0	41	108.57
2AT4P_R2_2	2E+05	2E+10	741	100	0	49	193.71
2AT4P_R2_3	2E+05	2E+10	846	100	0	56	237.07
4AT6P_R2_1	2E+05	2E+10	1065	100	0	22	16.16
4AT6P_R2_2	2E+05	2E+10	1041	100	0	22	32.44
4AT6P_R2_3	2E+05	2E+10	1044	100	0	28	33.32
8AT15P_R2_1	2E+15	2E+10	2752	100	0	30	30.83
8AT15P_R2_2	2E+15	2E+10	4176	100	0	29	101.05
8AT15P_R2_3	2E+15	2E+10	3932	100	0	34	61.32
15AT30P_R2_1	2E+20	2E+10	6024	100	0	54	418.85
15AT30P_R2_2	2E+20	2E+10	7680	100	0	61	1722.84
15AT30P_R2_3	2E+20	2E+10	249	100	0	57	7459.00
50AT100P_R2_1	2E+20	2E+10	x	0	x	55	>7200
50AT100P_R2_2	2E+20	2E+10	x	0	x	54	>7200
50AT100P_R2_3	2E+20	2E+10	x	0	x	56	>7200
100AT500P_R2_1	2E+30	2E+10	x	0	x	58	>7200
100AT500P_R2_2	2E+30	2E+10	x	0	x	58	>7200
100AT500P_R2_3	2E+30	2E+10	x	0	x	59	>7200
Average			**2090**	**71**	**0**	**43**	**>7200**

Table 4.7: Optimization results of MIBLP w/ batch optimization w/ relaxed time windows

Name	MIBLP w/o BO																
	β	M	Cost ($)	Service Rate (%)	Gap (%)	Optimization Horizon (min)	deltaT (min)	Total # of Batch	CPU Time (s)								
									Batch 1	Batch 2	Batch 3	Batch 4	Batch 5	Batch 6	Batch 7	Batch 8	Total
1AT2P_R1_1	2E+05	2E+03	313	100	0	22	15	1	1	x	x	x	x	x	x	x	1
1AT2P_R1_2	2E+05	2E+03	311	100	0	25	15	2	0.48	1.52	x	x	x	x	x	x	2
1AT2P_R1_3	2E+05	2E+03	327	100	0	20	15	1	1	x	x	x	x	x	x	x	1
2AT4P_R1_1	2E+03	5E+07	446	100	0	23	15	1	6.39	x	x	x	x	x	x	x	6.39
2AT4P_R1_2	2E+10	2E+05	428	100	0	21	10	2	6.15	x	7	x	x	x	x	x	13.15
2AT4P_R1_3	2E+10	2E+05	432	100	0	16	10	1	2.11	x	x	x	x	x	x	x	2.11
4AT6P_R1_1	2E+10	2E+05	820	100	0	57	5	3	17.79	7.39	x	x	11.19	x	x	x	36.37
4AT6P_R1_2	2E+10	2E+05	928	100	0	56	5	3	14.1	x	31.26	x	8.94	x	x	x	54.3
4AT6P_R1_3	2E+10	2E+05	821	100	0	38	10	2	74.17	78.37	x	x	x	x	x	x	152.54
8AT15P_R1_1	2E+15	2E+10	4559	100	0	49	10	2	113	2.92	x	x	x	x	x	x	115.92
8AT15P_R1_2	2E+15	2E+10	7394	100	0	42	5	3	47.32	9.78	33.4	x	x	x	x	x	90.5
8AT15P_R1_3	2E+15	2E+10	5716	100	0	43	10	2	102.55	1.31	x	x	x	x	x	x	103.86
15AT30P_R1_1	2E+20	2E+10	8086	100	0	62	5	5	34.8	1.68	2.21	247.71	4.21	x	x	x	290.61
15AT30P_R1_2	2E+20	2E+10	8777	100	0	80	10	4	85.44	20.38	3.84	8.52	x	x	x	x	118.18
15AT30P_R1_3	2E+20	2E+10	9479	100	0	100	10	5	17.07	3.45	102.9	10.33	7.71	x	x	x	141.46
50AT100P_R1_1	2E+20	2E+10	9444	89	0	61	3	8	116.35	14.06	59.78	1.2	1.93	10.81	5.02	17.21	226.36
50AT100P_R1_2	2E+20	2E+10	13083	85	0	60	5	5	25.08	17.66	81.25	1.05	3.68	x	x	x	128.72
50AT100P_R1_3	2E+20	2E+10	8319	85	0	54	2	8	4.75	14.25	14.48	0.57	1.06	1.61	4.55	19.48	60.75
200AT500P_R1_1	2E+20	2E+10	18764	87	0	115	7	6	102.49	137.46	31.09	59.76	18.86	27.29	x	x	201.65
200AT500P_R1_2	2E+20	2E+10	16547	73	0	103	10	5	72.39	113.11	28.56	46.9	51.31	x	x	x	215.4
200AT500P_R1_3	2E+20	2E+10	20178	82	0	128	6	7	98.58	31.52	151	103.47	21.4	20.82	28.27	x	265.83
Average			**6437**	**95**	**0**	**56**	**9**	**4**	**45**	**30**	**46**	**53**	**13**	**15**	**13**	**18**	**106.10**

Table 4.8: Optimization results of MIBLP w/ batch optimization w/ tight time windows

Name	MIBLP w/ BO																
	β	M	Cost ($)	Service Rate (%)	Gap (%)	Optimization Horizon (min)	deltaT (min)	Total # of Batch	CPU Time (s)								
									Batch 1	Batch 2	Batch 3	Batch 4	Batch 5	Batch 6	Batch 7	Batch 8	Total
1AT2P_R2_1	2E+05	2E+03	331	100	0	17	15	1	0.81	x	x	x	x	x	x	x	0.81
1AT2P_R2_2	2E+05	2E+03	422	100	0	9	15	2	0.08	1.32	x	x	x	x	x	x	1.4
1AT2P_R2_3	2E+05	2E+03	317	100	0	19	15	1	2.24	x	x	x	x	x	x	x	2.24
2AT4P_R2_1	2E+10	2E+05	446	100	0	19	5	1	6.39	x	x	x	x	x	x	x	6.39
2AT4P_R2_2	2E+10	2E+05	438	100	0	16	10	1	4.12	x	x	x	x	x	x	x	4.12
2AT4P_R2_3	2E+10	2E+05	432	100	0	16	5	1	2.11	x	x	x	x	x	x	x	2.11
4AT6P_R2_1	2E+10	2E+05	829	100	0	35	10	2	20.35	14.23	x	x	x	x	x	x	34.58
4AT6P_R2_2	2E+10	2E+05	736	100	0	16	10	1	18.65	x	x	x	x	x	x	x	18.65
5AT7P_R2_3	2E+05	2E+10	1395	100	0	68	10	3	39.55	0.85	139.84	x	x	x	x	x	180.24
8AT15P_R2_1	2E+15	2E+10	4422	100	0	68	5	3	91.7	70.81	x	7.68	x	x	x	x	170.19
8AT15P_R2_2	2E+10	2E+05	1519	100	0	82	10	3	19.8	27.41	x	5.19	x	x	x	x	52.4
8AT15P_R2_3	2E+10	2E+05	1732	100	0	64	10	3	41.27	69.1	16.78	x	x	x	x	x	127.15
15AT30P_R2_1	2E+20	2E+10	6611	100	0	42	10	3	100.88	21.39	20.06	x	x	x	x	x	142.33
15AT30P_R2_2	2E+20	2E+10	8601	100	0	61	5	5	14.84	5.14	6.19	1.36	3.64	x	x	x	31.17
15AT30P_R2_3	2E+20	2E+10	7832	100	0	58	5	5	25.74	1.01	1.94	3.74	2.13	x	x	x	34.56
50AT100P_R2_1	2E+20	2E+10	11757	100	0	70	5	5	15.4	17.62	6	8.77	14.39	x	x	x	62.18
50AT100P_R2_2	2E+20	2E+10	14450	100	0	56	5	5	12.36	2.99	3.74	5.53	24.45	x	x	x	49.07
50AT100P_R2_3	2E+20	2E+10	14831	92	0	59	3	8	17.81	8.31	32.1	12.48	13.32	3.77	6.75	24.07	118.61
200AT500P_R2_1	2E+20	2E+10	16786	86	0	115	8	7	130.26	66.39	15.78	28.88	10.33	9.85	12.39	x	273.88
200AT500P_R2_2	2E+20	2E+10	15673	80	0	83	10	4	122.38	37.5	66.16	43.37	x	x	x	x	269.41
200AT500P_R2_3	2E+20	2E+10	18934	89	0	113	6	8	113.46	57.85	61.33	51	17.99	13.09	10.45	6.78	331.95
Average			**6119**	**97**	**0**	**52**	**8**	**3**	**38**	**27**	**34**	**17**	**12**	**9**	**10**	**15**	**91.12**

Based on Tables VIII and IX, with tight time windows, the average cost is 4.94% lower, the average service rate is 2.8% higher, the average CPU time of each batch and the average total CPU time are less than those of relaxed time windows. Because relaxed time windows result in more possibilities, flexibility, and variables, it is reasonable that longer CPU time is needed. According to Tables VI to IX, the batch optimization technique with rolling horizons greatly reduces the CPU time and ensures that dynamic decisions can be made based on the optimization results of the previous batch (e.g., updated locations, passenger capacities, and statuses of the air taxis). For large-scale systems, we use batch optimization with rolling horizons to increase the computation efficiency by 98%. Overall, the results demonstrate that the optimal assignment between groups of users and air taxis and the optimal path of the air taxis can be found within two minutes on average. The largest problem size that the model can deal with includes 200 air taxis and 500 users by using a personal computer. When better computers are available, the CPU time can be further decreased, and the MIBLP model can handle larger-scale problems.

Table 4.9: Average service rate with different system dimensions

Number of Air Taxis	Number of Users	Average Service Rate (%)
1	2	100
2	4	100
4	6	100
8	15	100
15	30	100
50	100	92
200	500	83

In Table 4.9, we can see that the average service rate decreases when the problem size is large. The reasons are that (i) the number of air taxis is not enough to serve all the users with the latest pick-up and drop-off time constraints; (ii) the passenger capacity of each air taxis is randomly assigned to be two or four in every instance. The randomness of the initial total passenger capacity of all the air taxis leads to the insufficient resources of air taxis; and (iii) the average distance between the take-off and landing skyports is long among all the users so that it is more difficult for the air taxis to serve all the users within their maximum waiting time and arrival time constraints. The lowest average service rate is over 80% which is sufficient to ensure high service quality and user satisfaction.

4.3. Model Robustness

The parameters (β and *M*) need to be tuned to obtain feasible and optimal results. For each scenario, the optimal assignment and the optimal path of the air taxis will not change if we change β and *M*. However, different β and *M* will lead to different CPU time. If β is too small, the air taxi may not be assigned to any user. If *M* is too big, the optimization time will increase. In all, to obtain optimal results within a timely manner, β and *M* need to be tuned. According to Section IV-B, the value of *M* depends on the system dimension (i.e., the number of variables). In general, *M* is less than β (i.e., $M \approx \frac{\beta}{2}$), and β is much larger than the maximum value of the objective function (i.e., $\beta \gg Jmax$).

CHAPTER 5 CONCLUSIONS AND FUTURE RESEARCH

This work proposes a novel MIBLP model to optimize the multimodal transportation network of ground vehicles and air taxis with rolling-horizon batch optimization. This is one of the first works that integrates the ground transportation system with the AMoD system. Compared to other works, there are three important and distinct features of our MIBLP model: (i) the integration between the ground transportation system and the AMoD system; (ii) the combination of air taxi assignment and path planning problems; (iii) the electric energy consumption of the air taxis during different flight phases (take-off, in-flight, and landing); and (iv) the active and idle statuses of the air taxis are considered in the MIBLP model. The MIBLP model can find the cost-effective and real-time paths of the air taxi with respect to the number and locations of the air taxi and the information of the users' air taxi requests that include (i) pick-up and drop-off skyport locations, (ii) request time, (iii) maximum waiting time to be picked up, and (iv) maximum arrival time to be dropped off. By using Gurobi Optimizer, the MIBLP model has been validated to be able to efficiently solve ATAP in one mathematical model while optimizing the air taxi service with respect to service quality, operating cost, air taxi electric energy consumption, air taxi passenger capacity, and path capacity. For large-scale systems, we use batch optimization with rolling horizons to increase the computation efficiency by 98%. The MIBLP model needs to be tuned for model feasibility. The MIBLP model guarantees that air taxi requests are served within a timely manner, which means that the users will be picked up before the latest pick-up time and be dropped off before the latest drop-off time.

Due to the multimodal composition of the traveling process, the users' travel cost is affected by the ground and air traffic conditions which can be heavily uncertain. The uncertainties can come from cyber-attacks or miscommunication among the vehicles. These uncertainties will be addressed in the future work to ensure the resilient operation of the air taxi service. The operating cost and travel time between every two skyports are pre-assigned and remain static in our model. In the future work, the operating cost, travel time, and electric power of the air taxis will be dependent on the flight dynamics of the air taxis and the real-time air traffic conditions. We will also include the real-time ground traffic data into the mathematical model so that the ground travel time is more accurate, and the air taxi request time will be dependent on the real-time ground traffic conditions. Furthermore, after the optimal paths are found in the MIBLP model, we will use optimal control to design a control law to ensure that each air taxi follows its optimal path (i.e., reference path) with collision avoidance, to account for the safety concern. Since the configuration of the air taxi has not been finalized, we do not consider the aerodynamics of the air taxi, and so the collisions are not considered in this report. The future model will also account for different statuses (active, idle, maintenance check, or out-of-fuel/electricity) of the ground vehicles and the air taxis, to realize the optimal usage of the ground and aerial vehicles.

CHAPTER 6 SYNOPSIS OF PERFORMANCE INDICATORS

6.1. Part I of USDOT Performance Indicators

Two graduate students participated in the research project during the study period. The CCAT grant funds from this research project were used to support these two graduate students. One of the Ph.D. students graduated in May 2022, and the other student will graduate in May 2025.

6.2. Part II of USDOT Performance Indicators

Research Performance Indicator:

One conference presentation was produced from this project. The research from this advanced research project was disseminated to over 60 people in attendance (from industry, government, and academia) through the Next-generation Transport Systems Conference.

CHAPTER 7 STUDY OUTCOMES AND OUTPUTS

7.1. Output: Presentation

- Title of presentation: A Mixed Integer Bilinear Programming Model for Air Taxi Assignment and Path Planning
- Full Citation: Yang, S., Zhou, J., Sun, D., and DeLaurentis, D. (2023). "A Mixed Integer Bilinear Programming Model for Air Taxi Assignment and Path Planning," presented in-person at the 3rd Next Generation Transportation Systems Conference, West Lafayette, IN.

7.2. Outcomes

This project has the potential to bring several positive outcomes to society, especially in the context of urban mobility, transportation efficiency, environmental sustainability, and economic growth. Here are some potential outcomes:

- **Reduced Emissions and Environmental Impact:** By optimizing flight paths and assignments, the MIBLP model can help reduce the overall emissions and environmental impact of transportation vehicles. Electric or hybrid-electric air taxis could be used, contributing to lower carbon emissions and better air quality in urban environments.
- **Time Savings:** Efficient path planning and assignment can lead to significant time savings for commuters. This can enhance overall productivity and quality of life, as people spend less time in transit and have more time for work, leisure, and family activities.
- **Economic Growth and Innovation:** The development and implementation of air taxi services can stimulate economic growth by creating new industries, such as air taxi manufacturing, maintenance, and operation. This innovation can lead to job creation and increased economic activity.
- **Improved Accessibility:** Air taxis can provide an alternative mode of transportation for areas with limited infrastructure, such as remote or poorly connected regions. This can improve accessibility and connectivity, enabling people to access opportunities that were previously difficult to reach.
- **Reduced Congestion:** By offering an additional transportation option, air taxis can help reduce congestion on roads and highways. This can lead to smoother traffic flow and a reduction in the number of accidents caused by congestion-related factors.
- **Public Transportation Integration:** Air taxis can be integrated with existing public transportation systems, providing a seamless multimodal travel experience. This can encourage more people to use public transportation and reduce the dependence on private cars.
- **Technological Advancement:** The development and deployment of air taxis require advancements in aviation technology, including automation, communication systems, and

safety features. These technological advancements can have spillover effects in other industries and lead to further innovation.

- **Reduced Infrastructure Pressure:** As air taxis can utilize vertical takeoff and landing capabilities, they may require less ground infrastructure compared to traditional airports. This can alleviate the pressure on land use for expanding traditional airports.

It is important to note that while the potential outcomes are promising, the successful realization of these benefits depends on various factors, including regulatory approvals, public acceptance, safety considerations, technological advancements, and collaboration among stakeholders.

REFERENCES

[1] “Urban air mobility and advanced air mobility.” https://www.faa.gov/uas/advanced operations/urban air mobility/. Accessed: 2020-10-08.

[2] P. Whitley, “Unmanned aircraft system traffic management concept of operations version 2.”

[3] S. Rajendran and S. Srinivas, “Air taxi service for urban mobility: A critical review of recent developments, future challenges, and opportunities,” ArXiv, vol. abs/2103.01768, 2021.

[4] “Air taxis are about to change the future of travel.” https://www.slashgear.com/971155/air-taxis-are-about-to-change-the-future-of-travel/. Accessed: 2022-09-07.

[5] “Archer lands $1b order from united airlines and a spac deal.” https://techcrunch.com/2021/02/10/archer-lands-1-1b-order-from-united-airlines-and-a-spac-deal/. Accessed: 2022-09-07.

[6] “Archer electric vtol air taxi demo passes major test.” https://www.forbes.com/sites/edgarsten/2021/12/20/archer-air-taxi-demo-passes-major-test/?sh=f2da045411db. Accessed: 2022-09-07.

[7] “Boeing adds $450 million to air-taxi effort.” https://www.wsj.com/articles/boeing-expands-focus-on-air-taxis-11643022001. Accessed:2022-09-07.

[8] “American airlines invests in the future of urban air mobility.” https://news.aa.com/news/news-details/2021/American-Airlines-Invests-in-the-Future-of-Urban-Air-Mobility-FLT-06/default.aspx. Accessed: 2022-09-07.

[9] “Vx4: Faster, quieter, greener, cheaper.” https://vertical-aerospace.com/vx4/. Accessed: 2022-09-07.

[10] C. Riley, P. V. Hentenryck, and E. Yuan, “Real-time dispatching of large-scale ride-sharing systems: Integrating optimization, machine learning, and model predictive control,” ArXiv, vol. abs/2003.10942, 2020.

[11] J. Alonso-Mora, S. Samaranayake, A. Wallar, E. Frazzoli, and D. Rus, “On-demand high-capacity ridesharing via dynamic trip-vehicle assignment,” Proceedings of the National Academy of Sciences, vol. 114, p. 201611675, 01 2017.

[12] Z. Zhou and C. Roncoli, “A scalable vehicle assignment and routing strategy for real-time on-demand ridesharing considering endogenous congestion,” Transportation Research Part C: Emerging Technologies, vol. 139, p. 103658, 2022.

[13] M. Lokhandwala and H. Cai, “Dynamic ride sharing using traditional taxis and shared autonomous taxis: A case study of NYC,” Transportation Research Part C: Emerging Technologies, 2018.

[14] P. Pant and R. Harrison, “Estimation of the contribution of road traffic emissions to particulate matter concentrations from field measurements: A review,” Atmospheric Environment, vol. 77, p. 78–97, 10 2013.

[15] D. Milakis, B. Arem, and B. Wee, “Policy and society related implications of automated driving: A review of literature and directions for future research,” Journal of Intelligent Transportation Systems Technology Planning and Operations, vol. 21, pp. 324–348, 02 2017.

[16] L. Duan, Y. Wei, J. Zhang, and Y. Xia, “Centralized and decentralized autonomous dispatching strategy for dynamic autonomous taxi operation in hybrid request mode,” Transportation Research Part C-emerging Technologies, vol. 111, pp. 397–420, 2020.

[17] “Maker.” https://www.archer.com/maker. Accessed: 2022-09-07.

[18] R. Masson, F. Lehue´de´, and O. Pe´ton, “The dial-a-ride problem with transfers,” Computers & Operations Research, vol. 41, pp. 12–23, 2014.

[19] J.B.Greenblatt and S.Shaheen,“Automated vehicles, on-demand mobility, and environmental impacts,” Current Sustainable/Renewable Energy Reports, vol. 2, no. 3, pp. 74–81, 2015.

[20] H. Wang and H. Yang, “Ridesourcing systems: A framework and review,” Transportation Research Part B: Methodological, vol. 129,pp. 122–155, 2019.

[21] L. FRANCKX, “What are ridesourcing / transportation network company (TNC) services?” https://mobilitybehaviour.eu/2017/07/26/what-are-ridesourcingtransportation-network-company-tnc-services/. Accessed: 2023-02-08.

[22] R. K. Pant, S. D. Gogate, and P. Arora, “Economic parameters in the conceptual design optimization of an air-taxi aircraft,” Journal of aircraft, vol. 32, no. 4, pp. 696–702, 1995.

[23] G. Guruswamy, “Computation of gust induced responses of an air taxi by using navier-stokes equations,” Aerospace science and technology, vol. 127, pp. 107684–, 2022.

[24] A.Akash, V.S.J.Raj, R.Sushmitha, B.Prateek, S.Aditya, and V.M.Sreehari, “Design and analysis of VTOL operated intercity electrical vehicle for urban air mobility,” Electronics (Basel), vol. 11, no. 1, pp. 20–, 2021.

[25] A. Brown and W. Harris, “Vehicle design and optimization model for urban air mobility,” Journal of Aircraft, vol. 57, pp. 1–11, 10 2020.

[26] A. Datta, S. Elbers, S. Wakayama, J. Alonso, E. Botero, C. Carter, and F. Martins, “Commercial intra-city on-demand electric-VTOL status of technology,” NASA Aeronautics Research Institute, Technical Report TVF WG, vol. 2, 2018.

[27] A. Bacchini and E. Cestino, “Electric VTOL configurations comparison,” Aerospace, vol. 6, no. 3, p. 26, 2019.

[28] J. Enconniere, J. Ortiz-Carretero, and V. Pachidis, “Mission performance analysis of a conceptual coaxial rotorcraft for air taxi applications,” Aerospace Science and Technology, vol. 69, pp. 1–14, 2017.

[29] M. Rimjha, S. Hotle, A. Trani, and N. Hinze, “Commuter demand estimation and feasibility assessment for urban air mobility in northern California,” Transportation research. Part A, Policy and practice, vol. 148, pp. 506–524, 2021.

[30] R. Goyal, C. Reiche, C. Fernando, and A. Cohen, “Advanced air mobility: Demand analysis and market potential of the airport shuttle and air taxi markets,” Sustainability (Basel, Switzerland), vol. 13, no. 13, pp. 7421–, 2021.

[31] L. Garrow, B. German, P. Mokhtarian, and J. Glodek, “A survey to model demand for eVTOL urban air trips and competition with autonomous ground vehicles,” 06 2019.

[32] K. Becker, I. Terekhov, and V. Gollnick, “A global gravity model for air passenger demand between city pairs and future interurban air mobility markets identification,” 06 2018.

[33] H. Shin, T. Lee, and H.-R. Lee, “Skyport location problem for urban air mobility system,” Computers & operations research, vol. 138, pp. 105611–, 2022.

[34] S. Rath and J. Y. Chow, “Air taxi skyport location problem with single-allocation choice-constrained elastic demand for airport access,” Journal of air transport management, vol. 105, 2022.

[35] S. Rajendran and J. Zack, “Insights on strategic air taxi network infrastructure locations using an iterative constrained clustering approach,” Transportation Research Part E: Logistics and Transportation Review, vol. 128, pp. 470–505, 2019.

[36] A. Bozorgi-Amiri, S. Tavakoli, H. Mirzaeipour, and M. Rabbani, “Integrated locating of helicopter stations and helipads for wounded transfer under demand location uncertainty,” The American Journal of Emergency Medicine, vol. 35, no. 3, pp. 410–417, 2017.

[37] S. Rath and J. Y. Chow, “Air taxi skyport location problem with single-allocation choice-constrained elastic demand for airport access,” Journal of Air Transport Management, vol. 105, p. 102294, oct 2022.

[38] N.Agatz, A.Erera,M.Savelsbergh, and X.Wang, “Optimization for dynamic ride-sharing: A Review,”European Journal of Operational Research, vol. 223, no. 2, pp. 295–303, 2012.

[39]E. O ̈zkan and A.R.Ward, “Dynamic matching for real-time ridesharing,” Stochastic Systems, vol.10, no.1, pp.29–70, 2020.

[40] A. Najmi, D. Rey, and T. H. Rashidi, “Novel dynamic formulations for real-time ride-sharing systems,” Transportation research part E: logistics and transportation review, vol. 108, pp. 122–140, 2017.

[41] C. Yan, H. Zhu, N. Korolko, and D. Woodard, “Dynamic pricing and matching in ride-hailing platforms,” Naval Research Logistics (NRL), vol. 67, no. 8, pp. 705–724, 2020.

[42] D.-S. Jang, C. Ippolito, S. Sankararaman, and V. Stepanyan, “Concepts of airspace structures and system analysis for uas traffic flows for urban areas,” 2017.

[43] T. Prevot, J. Rios, P. Kopardekar, J. Robinson III, M. Johnson, and J. Jung, “UAS traffic management (utm) concept of operations to safely enable low altitude flight operations,” 06 2016.

[44] N. Pongsakornsathien, S. Bijjahalli, A. Gardi, A. Symons, Y. Xi, R. Sabatini, and T. Kistan, “A performance-based airspace model for unmanned aircraft systems traffic management,” Aerospace, vol. 7, no. 11, pp. 154–, 2020.

[45] N. Labib, G. Danoy, J. Musial, M. Brust, and P. Bouvry, “Internet of unmanned aerial vehicles—a multilayer low-altitude airspace model for distributed UAV traffic management,” Sensors, vol. 19, p. 4779, 11 2019.

[46] S. Rajendran and J. Shulman, “Study of emerging air taxi network operation using discrete-event systems simulation approach,” Journal of Air Transport Management, vol. 87, p. 101857, 2020.

[47] A. Straubinger, R. Rothfeld, M. Shamiyeh, K.-D. Buchter, J. Kaiser, and K. O. Plotner, “An overview of current research and developments in urban air mobility – setting the scene for UAM introduction,” Journal of Air Transport Management, vol. 87, p. 101852, 2020.

[48] T. Cetin and E. Deakin, “Regulation of taxis and the rise of ridesharing,” Transport Policy, vol. 76, pp. 149–158, 2019.

[49] H. Zhang, J. Chen, W. Li, X. Song, and R. Shibasaki, “Mobile phone GPS data in urban ridesharing: An assessment method for emission reduction potential,” Applied Energy, vol. 269, p. 115038, 2020.

[50] H. Bian, Q. Tan, S. Zhong, and X. Zhang, “Assessment of UAM and drone noise impact on the environment based on virtual flights,” Aerospace science and technology, vol. 118, pp. 106996–, 2021.

[51] A. Straubinger, E. T. Verhoef, and H. L. de Groot, “Will urban air mobility fly? the efficiency and distributional impacts of UAM in different urban spatial structures,” Transportation research. Part C, Emerging technologies, vol. 127, pp. 103124–, 2021.

[52] J. Wang, M. K. Lim, Y. Zhan, and X. Wang, “An intelligent logistics service system for enhancing dispatching operations in an IOT environment,” Transportation Research Part E: Logistics and Transportation Review, vol. 135, p. 101886, 2020.

[53] Z. Zhang, J. Wu, J. Dai, and C. He, “A novel real-time penetration path planning algorithm for stealth UAV in 3d complex dynamic environment,” IEEE Access, vol. 8, pp. 122757–122771, 2020.

[54] J. Tisdale, Z. Kim, and J. K. Hedrick, “Autonomous UAV path planning and estimation,” IEEE Robotics & Automation Magazine, vol.16, no. 2, pp. 35–42, 2009.

[55] V. Roberge, M. Tarbouchi, and G. Labonte, “Comparison of parallel genetic algorithm and particle swarm optimization for real-time UAV path planning,” IEEE Transactions on Industrial Informatics, vol. 9, no. 1, pp. 132–141, 2013.

[56] J. Tordesillas, B. T. Lopez, and J. P. How, “Faster: Fast and safe trajectory planner for flights in unknown environments,” 2019.

[57] D. Falanga, P. Foehn, P. Lu, and D. Scaramuzza, “Pampc: Perception-aware model predictive control for quadrotors,” 2018.

[58] J. Tordesillas and J. P. How, “Mader: Trajectory planner in multi-agent and dynamic environments,” 2020.

[59] A. Pimpinella, A. E. Redondi, and M. Cesana, “Walk this way! an IOT-based urban routing system for smart cities,” Computer Networks, vol. 162, p. 106857, 2019.

[60] Z. Fu, J. Yu, G. Xie, Y. Chen, and Y. Mao, “A heuristic evolutionary algorithm of UAV path planning,” Wireless Communications and Mobile Computing, vol. 2018, pp. 1–11, 09 2018.

[61] A. Mardani, M. Chiaberge, and P. Giaccone, “Communication-aware UAV path planning,” IEEE Access, vol. 7, pp. 52609–52621, 2019.

[62] H. Shiri, J. Park, and M. Bennis, “Remote UAV online path planning via neural network based opportunistic control,” 2019.

[63] P. Yao, H. Wang, and Z. Su, “Real-time path planning of unmanned aerial vehicle for target tracking and obstacle avoidance in complex dynamic environment,” Aerospace Science and Technology, vol. 47, pp. 269–279, 2015.

[64] Z. Yuan, Y. Yang, Y. Hu, and X. Ma, “Channel-aware potential field trajectory planning for solar-powered relay UAV in near-space,” IEEE Access, vol. 8, pp. 143950–143961, 2020.

[65] C. Riley, P. V. Hentenryck, and E. Yuan, “Real-time dispatching of large-scale ride-sharing systems: Integrating optimization, machine learning, and model predictive control,” ArXiv, vol. abs/2003.10942, 2020.

[66] J. Alonso-Mora, S. Samaranayake, A. Wallar, E. Frazzoli, and D. Rus, “On-demand high-capacity ridesharing via dynamic trip-vehicle assignment,” Proceedings of the National Academy of Sciences of the United States of America, vol. 114, pp. 462 – 467, 2017.

[67] G. Guo and Y. Xu, “A deep reinforcement learning approach to ride-sharing vehicle dispatching in autonomous mobility-on-demand systems,” IEEE Intelligent Transportation Systems Magazine, vol. 14, no. 1, pp. 128–140, 2022.

[68] A. Fielbaum, X. Bai, and J. Alonso-Mora, “On-demand ridesharing with optimized pick-up and drop-off walking locations,” Transportation Research Part C: Emerging Technologies, vol. 126, p. 103061, 2021.

[69] S. Chen, H. Wang, and Q. Meng, “Solving the first-mile ridesharing problem using autonomous vehicles,” Computer-Aided Civil and Infrastructure Engineering, vol. 35, 06 2019.

[70] M. Zhao, J. Yin, S. An, J. Wang, and D. Feng, “Ridesharing problem with flexible pickup and delivery locations for app-based transportation service: Mathematical modeling and decomposition methods,” Journal of Advanced Transportation, vol. 2018, pp. 1–21, 07 2018.

[71] J. Alonso-Mora, S. Samaranayake, A. Wallar, E. Frazzoli, and D. Rus, “On-demand high-capacity ridesharing via dynamic trip-vehicle assignment,” Proceedings of the National Academy of Sciences, vol. 114, no. 3, pp. 462–467, 2017.

[72] D. J. Fagnant and K. M. Kockelman, “Dynamic ridesharing and fleet sizing for a system of shared autonomous vehicles in Austin, Texas,” Transportation, vol. 45, no. 1, pp. 143–158, 2018.

[73] R. Dai, C. Ding, J. Gao, X. Wu, and B. Yu, “Optimization and evaluation for autonomous taxi ride-sharing schedule and depot location from the perspective of energy consumption,” Applied Energy, 2022.

[74] W. Chen, M. Mes, M. Schutten, and J. Quint, “A ride-sharing problem with meeting points and return restrictions,” Transportation Science, vol. 53, 01 2019.

[75] J. Ma, X. Li, F. Zhou, and W. Hao, “Designing optimal autonomous vehicle sharing and reservation systems: A linear programming approach,” Transportation Research Part C: Emerging Technologies, vol. 84, pp. 124–141, 2017.

[76] H. Hosni, J. Naoum-Sawaya, and H. Artail, “The shared-taxi problem: Formulation and solution methods,” Transportation Research Part B: Methodological, vol. 70, pp. 303–318, 2014.

[77] M. MARKO, “Yellow flying taxi isolated on white background, city electric transport drone.,” 2020. [Online; accessed June 27, 2022].

[78] O. Toker and H. Ozbay, “On the np-hardness of solving bilinear matrix inequalities and simultaneous stabilization with static output feedback,” in Proceedings of 1995 American Control Conference - ACC’95, vol. 4, pp. 2525–2526 vol.4, 1995.

[79] V. Blondel and J. Tsitsiklis, “Np-hardness of some linear control design problems,” in Proceedings of 1995 34th IEEE Conference on Decision and Control, vol. 3, pp. 2910–2915 vol.3, 1995.

[80] “Gurobi optimizer.” https://www.gurobi.com/events/solving-bilinear-programming-problems/. Accessed: 2022-05-05.

[81] M. Cococcioni and L. Fiaschi, “The big-m method with the numerical infinite m,” Optim. Lett., vol. 15, pp. 2455–2468, 2021.

[82] E. Ubi, “A three-phase simplex method for infeasible and unbounded linear programming problems,” Journal of Mathematical and Computational Science, 2020.

[83] T. Ding, R. Bo, W. Gu, and H. Sun, “Big-m based MIQP method for economic dispatch with disjoint prohibited zones,” IEEE Transactions on Power Systems, vol. 29, pp. 976–977, 2014.